Analyst

Rapid Quantification of microRNA-375 through One-Pot Primer-Generating Rolling Circle Amplification

Journal:	*Analyst*
Manuscript ID	AN-COM-02-2022-000263.R1
Article Type:	Communication
Date Submitted by the Author:	15-May-2022
Complete List of Authors:	Smith, Lucas; University of Illinois Urbana-Champaign, Bioengineering Nalla, Siva; University of Illinois Urbana-Champaign, Bioengineering Kuo, Chia-Wei; University of Illinois Urbana-Champaign, Bioengineering Kohli, Manish; University of Utah Health Huntsman Cancer Institute, Division of Oncology Smith, Andrew; University of Illinois Urbana-Champaign, Bioengineering

Rapid Quantification of microRNA-375 through One-Pot Primer-Generating Rolling Circle Amplification

Lucas D. Smith,[1,2] Siva Nalla,[1,2] Chia-Wei Kuo,[1,2] Manish Kohli,[3,4] and Andrew M. Smith[1,2,4,5,6,7*]

[1] Department of Bioengineering, University of Illinois Urbana-Champaign, Urbana, Illinois 61801, USA

[2] Micro and Nanotechnology Laboratory, University of Illinois Urbana-Champaign, Urbana, Illinois 61801, USA

[3] Division of Oncology, Huntsman Cancer Institute, University of Utah, Salt Lake City, UT 84112 USA

[4] Carl R. Woese Institute for Genomic Biology, University of Illinois Urbana-Champaign, Urbana, Illinois 61801, USA

[5] Department of Materials Science & Engineering, University of Illinois Urbana-Champaign, Urbana, Illinois 61801, USA

[6] Cancer Center at Illinois, University of Illinois Urbana-Champaign, Urbana, IL 61801 USA

[7] Carle Illinois College of Medicine, Urbana, Illinois 61801, USA

* To whom correspondence should be addressed: smi@illinois.edu

Abstract

A recent surge of interest in microRNA has been driven by their discovery as circulating biomarkers of disease, with many diagnostic test platforms currently under development. Alternatives to widely used microRNA quantification methods such as quantitative reverse transcriptase PCR (qRT-PCR) are needed for use in portable and point-of-care devices which are incompatible with complex sample processing workflows and thermal cycling. Rolling circle amplification (RCA) is a one-pot assay technique which directly amplifies nucleic acids using sequence-specific microRNA priming to initiate a single-step isothermal reaction and is compatible with simple devices. Sensitivity remains a limitation of RCA methods, however, and detection limits do not typically reach the femtomolar level in which microRNA targets are present in blood. RCA assays have previously been improved by digestion of the amplification products using a nicking endonuclease to exponentially generate new reaction primers. Here we describe how a ligation-free version of this technique performed in a single tube can be used to improve the limit of detection for microRNA-375, an important blood biomarker for prostate cancer. Endonuclease addition changes a linear process into an exponential amplification reaction which results in a 61-fold improvement of the limit of detection (5.9 fM), a dynamic range wider than 5-log(10), and a shorter reaction time. By eliminating the need for microRNA reverse transcription and thermal cycling, this single-step, one-pot method provides a more rapid and simplified alternative to qRT-PCR for ultrasensitive microRNA quantification in blood extract, which we anticipate will provide a convenient, ultrasensitive, and easily automated platform for microRNA biomarker analysis.

Keywords

prostate cancer, point of care, miR-375, RNA, fluorescence, enzyme, polymerase, nickase

MicroRNAs (miRs) are short non-coding RNAs that function as conserved genetic regulatory elements. These molecules were discovered in *Caenorhabditis elegans* in the early 1990s[1] and were later identified as essential determinants of gene expression and phenotype in a wide range of organisms.[2] Over the past decade, miRs have been shown to be biochemical drivers of disease and potential clinical diagnostic and prognostic indicators of numerous clinical conditions. A particularly promising application is for early detection and monitoring of cancer using circulating blood-borne miRs.[3,4] Circulating miR sequences have been identified that correlate with clinical indications of each of the most common types of cancer.[5,6] One example is miR-375, which was discovered through sequencing of blood exosomal miR to be a prognostic biomarker of treatment outcome for advanced stage prostate cancer at the castration resistance stage.[4] Animal models indicate that miR-375 mediates apoptotic response, cell differentiation, and chemotherapy resistance, making its detection appealing for guiding clinical treatment decisions.[3-7]

While no FDA-approved tests are currently in use for detecting circulating miR, there is widespread interest in developing such tests. A variety of assays have been used to detect and quantify miR, each with advantages and limitations for specific applications. In research laboratory settings, microarrays, RNA sequencing (RNA-Seq), and quantitative reverse transcriptase polymerase chain reaction (qRT-PCR) are the most common methods, and are each available as commercial kits.[8,9] Microarrays allow multiplexed detection, but high cost, low sensitivity, low adaptability to new targets, and high false positive rates make them inappropriate for routine testing.[9] Alternatively, RNA-Seq allows identification of novel miRs with high sensitivity, but costs are much higher than other methods and considerable data analysis hinders applications in routine clinical settings. Clinical applications of miR detection typically require analyses of only a small number of established sequences with low cost and high throughput. Such medical applications also demand high sensitivity, specificity, reproducibility, and speed, making qRT-PCR an attractive option.[8,9] While qRT-PCR and its digital variants are gold standards of sensitivity for long RNAs, challenges remain for assays targeting short miRs.[8,9] Moreover, a contemporary trend is the miniaturization and simplification of rapid molecular assays for use at the point-of-care in clinics or low-resource settings, scenarios in which PCR-based methods remain incompatible due to the need for precise thermal cycling.[10]

Rolling circle amplification (RCA) is a promising method to address current limitations of miR quantification. With RCA, a miR target is simply mixed with a solution containing a complimentary circular single-stranded DNA (ssDNA) template, polymerase, deoxynucleotide

triphosphates (dNTPs), and activatable fluorescent probes such as DNA-binding dyes. The polymerase synthesizes ssDNA appended to the miR as it propagates repeatedly around the circular template to generate long nucleic acids, measured by fluorescent probe signal. This process proceeds in an isothermal manner without the need for a thermocycler, providing a simple one-pot procedure that is conducive to point-of-care devices.[11]

Challenges remain with RCA methods, however. Simplified protocols have been developed to detect miRs using isothermal RCA with fluorescent probes or molecular beacons, but these methods achieve picomolar detection limits, which are orders of magnitude higher than clinical levels of miR biomarkers.[12] Similar detection limits also result when RCA is preceded by padlock probe ligation to circularize templates with sequence specificity to the target miR.[13] In contrast to PCR-based methods which result in exponential nucleic acid amplification, the sensitivity RCA-based methods is limited by the linear nucleic acid amplification. To improve detection limits, methods have been developed to enzymatically nick RCA amplicons to generate new templates which can be used for template ligation, which results in exponential growth of nucleic acids and an exponential increase in detected signals. This strategy was originally developed to isothermally amplify DNA[14] and was later applied to detect messenger RNA[15] and miR,[16] increasing assay sensitivity in all cases, but with increasingly complex reagent design and assay workflows. In particular, the need for both ligation and RCA steps in each amplification cycle limits reaction rates relative to a single-step exponential process. Alternatively, a variety of strategies have been explored for detection of miR at the single molecule level, but these require secondary labeling steps, expensive equipment, and data post-processing that are not compatible with portable instruments with simple readouts.[12,17]

In this letter, we show that a one-pot RCA reaction containing a nicking endonuclease can be optimized to improve the limit of detection of miR-375 by orders of magnitude and to expand the detection range to achieve exponential amplification without the need for ligation steps. The reaction is depicted in **Figure 1**, showing polymerase-mediated extension of the miR using a circular DNA, resulting in linear extension of the miR target as ssDNA concatemers that are complimentary to the circular template sequences. Additional circular DNAs bind to the extended molecule to generate double-stranded DNA (dsDNA) restriction sites for endonucleases. The nicking endonuclease introduces single-stranded breaks in the concatemer, yielding additional molecules that serve as primers capable of initiating independent RCA reactions. This primer-generating RCA process (pg-RCA) converts the enzymatic process from one that linearly generates DNA to one with exponential growth. DNA

can then be quantified in real time by monitoring the fluorescence of DNA-specific dyes using a widely available qPCR instrument.[17] This assay occurs rapidly at a constant temperature in a single pot, with substantially lower process complexity than qRT-PCR, but with a similar data readout.[14]

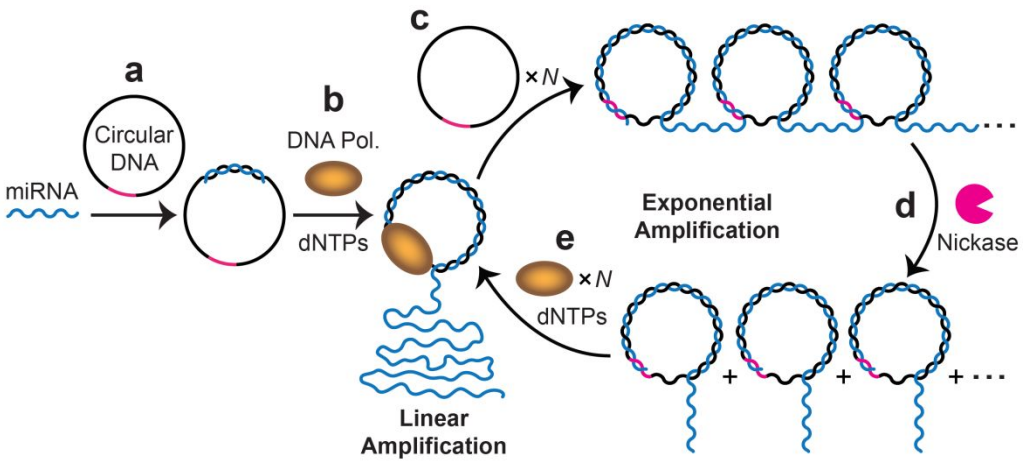

Figure 1. Schematic depiction of miR-primed RCA. (a) A miR target hybridizes with a circular DNA template with complementary sequence. The template contains a sequence specific for the nickase Nb.BbvCI (pink). **(b)** The miR serves as a primer for RCA using Φ29 DNA polymerase, resulting in DNA synthesis at a rate linearly proportional to the number of miR targets. **(c)** Extended RCA products hybridize with additional DNA templates. **(d)** Single-stranded breaks are introduced in the amplicon strand by the nickase, resulting in separate molecules. **(e)** Each molecule can initiate new RCA reactions, yielding exponential signal amplification.

Results and Discussion

pg-RCA Assay Design. We designed a 79-base circular ssDNA template (**Figure S1**) to contain both a complementary sequence to the full-length 22-mer miR-375 target as well as a 7-base recognition site for the nickase Nb.BbvCI (**Table S1**). The template sequence was designed based on studies indicating that polymerase activity varies sinusoidally with template length[18] and that templates with high AC content facilitate faster amplicon generation.[19] The nickase recognition site is adjacent to the miR binding site to allow future performance tests related to the modularity of the larger non-complimentary spacer region. The linear template was synthesized with a 5' phosphoryl group and circularized using CircLigase II, which specifically catalyzes intramolecular phosphodiester bond formation. Exonuclease I, a ssDNA-

specific nuclease, was used to digest non-circularized nucleic acids, confirmed by polyacrylamide gel electrophoresis (**Figure S2**). Solutions containing miR sequences were added to a tube containing the circular template, dNTPs, and an amplification reaction mixture containing Φ29 polymerase.[14] ssDNA synthesis was quantified in real time by measuring fluorescence from the DNA intercalating SYBR Gold dye, and a fluorescence intensity threshold was applied to calculate the time to generate detectable DNA products. This cutoff time was then correlated with target concentration.

RCA Product Characterization. Reactions were performed using conventional linear RCA and exponential pg-RCA with miR-375 concentrations spanning 10 fM to 10 nM in log(10) increments. Agarose gel electrophoresis of products demonstrated that the major fraction of linear RCA products were polydisperse and much larger than the largest dsDNA marker (48 kbp), with the major fraction unable to penetrate into the gel (**Figure 2**). Size distributions across all miR-375 concentrations were similar, with substantially reduced signal for miR concentrations less than 100 pM. In contrast, exponential pg-RCA reaction products were smaller and more uniform in size, with a primary migration band corresponding to a 50 kbp product for all concentrations. The vast majority of pg-RCA products entered the gel except for a small fraction in the 10 nM sample. Products were detectable in the gel for miR-375 concentrations as low as 10 pM. The fact that DNA products from nickase reactions remain large suggests that the reaction conditions facilitate an RCA polymerization process that is considerably faster than the rates of hybridization of additional circular templates and/or nicking of dsDNA endonuclease sites.

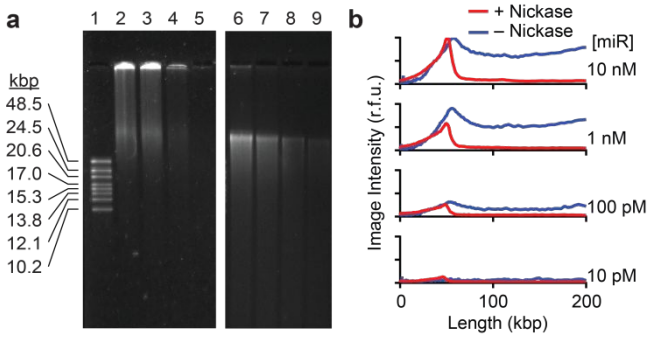

Figure 2. Agarose gel electrophoresis of RCA products. (a) Gels stained with SYBR Gold. Lanes contain: (1) dsDNA ladder; (2–5) linear RCA products; (6–9) pg-RCA products. Reactions contain miR-375 at (2,6) 10 nM, (3,7) 1 nM, (4,8) 100 pM, or (5,9) 10 pM. Full gels and analyses are shown in **Figures**

S3 and **S4**. **(b)** Product length distributions based on fluorescence intensity. Length was calibrated by fitting of dsDNA migration distance to known length for each ladder band ($R^2 > 0.99$).

Reaction Condition Optimization. Reaction parameters were optimized based on reaction rates from SYBR Gold fluorescence over 4 hours using a qPCR instrument.[20] Reactions were performed with 1 pM and 0 pM miR-375 to identify parameters that maximize target-specific signal and minimize fluorescence generated in the absence of the target deriving from spontaneous amplification, which is the current limitation of RCA for low concentration samples. With increasing nickase concentration, fluorescence was detectable more rapidly (**Figure S5a** and **S5e**). Without nickase, negligible signal was measured for nearly 4 hours, whereas at high concentrations, signal was detectable above intensity thresholds within 1 hour (raw data are shown in **Figure S6a** and **S6d**). Similarly, increasing polymerase concentration with constant nickase concentration shortened the reaction time, with fast and similar rates above 0.015 U μL^{-1} (**Figures S5b**, **S5f**, **S6a**, and **S6d**). The circular template concentration endowed the highest degree of reaction rate tunability (**Figure S5c** and **S5g**), reducing reaction times for 1 pM miR-375 to less than 1 hour at template concentrations higher than 1 nM. Notably, increasing the circular template concentration led to an abrupt intensity rise consistent with exponential DNA growth (**Figure S6c** and **S6f**). For all three reaction components, decreasing concentration increased the signal-to-background such that the maximum difference between the 0 pM and 1 pM miR-375 solutions was achieved at lower concentrations (**Figure S5** and **S6**), which can likely be attributed to the greater temporal resolution for longer reaction times. Indeed, intensity differences between samples containing 0 pM and 1 pM miR-375 increased over time using reagent concentrations optimized for maximum sensitivity (**Figure S5d** and **S5h**). Longer reaction times are therefore useful to yield specific signals in low concentration samples, but the nickase, polymerase, and circular template concentrations can be tuned to decrease reaction times for more sensitive instruments in which lower signals are measurable.

***Analytical Assay Performance*.** We applied reaction parameters optimized for enhanced assay sensitivity for the quantification of miR-375 using one-pot RCA. RCA reactions performed in the absence of nickase (**Figure 3a**) showed an increase in fluorescence as a function of reaction time, with samples containing higher miR-375 concentrations exhibiting faster rates of increase (higher slope). Applying the same intensity threshold to each time-course over the 4 hour reaction resulted in an assay with dynamic range spanning 3-log(10) values of

concentration with a lower limit of detection of 223 fM (**Figure 3b**), which is an improvement in sensitivity compared with prior reports for linear RCA.[21] Fluorescence intensity trajectories were markedly different when reactions were performed in the presence of nickase (**Figure 3c**), which resulted in sigmoidal curves with enhanced offsets in the time to detect amplification. These amplification profiles are consistent with an exponential growth trend. The intensity time courses for pg-RCA also exhibited lower intensity variations between technical replicates, as indicated by line width, when compared with linear RCA, as a result of the increased fluorescence intensity observed in exponential pg-RCA. The average coefficient of variation of intensity cutoff times for pg-RCA reactions was 0.60%, compared with 6.85% for linear RCA reactions. Most importantly, sensitivity at lower target concentrations increased markedly (**Figure 3d**), leading to a 61-fold improvement in the lower limit of detection (5.9 fM) and a dynamic range spanning more than a 5-log(10) concentration range. The combination of high analytical sensitivity and wide dynamic range is particularly important due to the large variation in miR concentrations in biological fluids with lower limits in the femtomolar range in clinical plasma samples.[22]

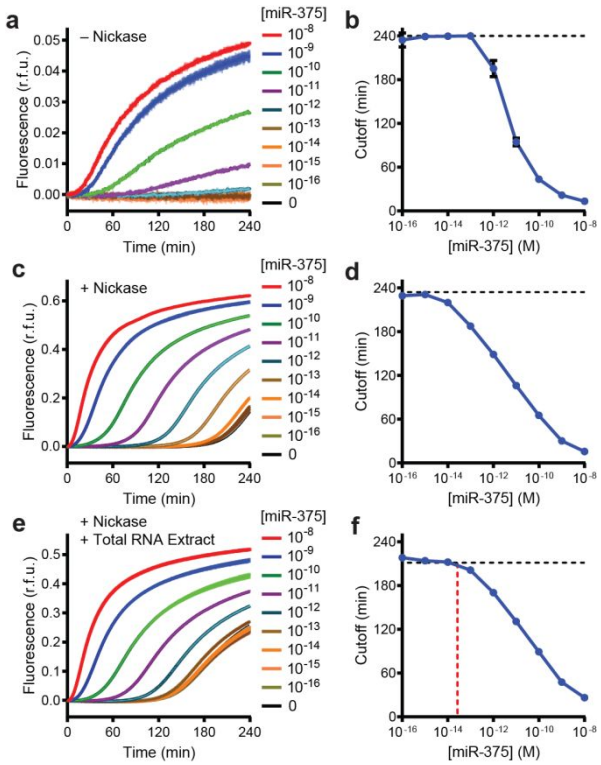

Figure 3. miR-375 detection by real-time RCA fluorescence. (a,c,e) Reactions were monitored by SYBR Gold emission in a qPCR instrument. **(b,d,f)** Cutoff time as a function of miR-375 concentration. Data are averages of 3 technical replicates. Line width or error bar indicates standard deviation. Dashed

black lines are cutoff times for samples with 0 miR. **(a,b)** Linear RCA. **(c,d)** pg-RCA in buffer. **(e,f)** pg-RCA in human plasma RNA extract. Results were similar when trajectories were analyzed by endpoint fluorescence (**Figure S7**).

To verify assay function for detection of native miR-375 in a representative medical biospecimen containing a complex matrix, pg-RCA was performed using TRIzol-extracted RNA from human plasma.[24] To calibrate with an internal reference, synthetic miR-375 was spiked into the extract at known concentrations. **Figure 3e** shows that the reactions were similar in exponential trends to those performed in buffer alone. **Figure 3f** shows that the target could be detected over a dynamic range of 4-log(10) concentration. A linear interpolation of the dynamic range to the baseline led to a measurement of 47 fM miR-375. This value is consistent with the expected miR-375 concentration in healthy human plasma RNA extracts and represents a value below the limit of detection of linear RCA.

We further validated the sequence specificity of pg-RCA optimized for miR-375 detection by evaluating signals from reactions using a scrambled target sequence and miR-375 isoforms (**Figure S8**). We tested the four most prevalent miR-375 isomiRs (miR-375.1, miR-375.2, miR-375.3, miR-375.4) found from next-generation sequencing of exosomal RNA extracts from human plasma (**Table S1**).[23] The most prevalent miR-375 isomiR, miR-375.1, generated the shortest pg-RCA cutoff time. The other miR-375 isoforms yielded significantly longer cutoff times, which is consistent with the design of the circular template binding site for miR-375.1. The shorter regions of complementarity and sequence mismatch for the less prevalent isomiRs should reduce binding and thereby reduce priming of amplification. The scrambled sequence resulted in a measured effective target concentration that was 66-fold lower than that of miR-375.1. Together, these data provide evidence that this one-pot pg-RCA assay enables detection and quantification of endogenous miR-375 in the presence of excess off-target RNA using a simple and rapid reaction protocol.

Conclusions

miRs have been identified as significant clinical biomarkers for a variety of diseases.[3-7] Despite broad interest and urgent needs in medical and academic communities, however, gold standard miR quantification methods require lengthy detection protocols that may introduce biases and

delays in receiving results. Further, multistep protocols are not conducive to point-of-care applications and introduce additional barriers for automation. In this study, we demonstrated a single-step one-pot assay to exponentially amplify miR-375 signals using pg-RCA. This method provides a sensitive, simplified, and user-friendly alternative to qRT-PCR for the quantification of low abundance miRs, is compatible with complex biospecimens, and achieves a lower limit of detection of 5.9 fM and a 5-log(10) detection range. We anticipate that this technique can be used in conjunction with other emerging technologies including digital droplet assays as well as point-of-care devices that benefit from simplified reaction protocols and isothermal conditions.

Methods

Chemicals and Reagents. DNA and RNA oligonucleotides with sequences shown in **Table S1** were purchased from Integrated DNA Technologies. The oligos were resuspended in molecular biology grade water (Corning), centrifuged (5 min, 5000*g*), characterized for concentration and purity based on absorption at wavelengths of 260 nm and 280 nm, and stored at –20 °C. CircLigase II was purchased from Lucigen. Deoxynucleotide Solution Mix (dNTPs), Φ29 DNA polymerase, and *E. coli* Exonuclease I were purchased from New England Biolabs. SYBR Gold Nucleic Acid Gel Stain (SYBR Gold), and TRIzol LS Reagent were purchased from ThermoFisher Scientific. Mini-PROTEAN Tris/Borate/EDTA (TBE) Urea Gel (10%), 2× TBE-Urea sample buffer, and 10× TBE Urea were purchased from Bio-Rad Laboratories. Phosphate buffered saline (PBS) was purchased from Corning. In-house purified Milli-Q water was used throughout. Unless specified, all other chemicals and solvents were purchased from Sigma-Aldrich and used without further purification.

Circular Template Synthesis. The linear pg-RCA template (500 nM, **Table S1**) with 5'-phosphoryl modification was circularized using CircLigase II (10 U μL^{-1}) in 0.33 M Tris-acetate, 0.66 M potassium acetate, 2.5 mM $MnCl_2$, 1 M betaine, and 5 mM dithiothreitol at pH 7.5 for 2 hr at 60 °C. Unreacted linear DNA was degraded by reaction with Exonuclease I for 2 hr at 37 °C before a 10 min incubation at 80 °C.

***pg-RCA*.** A 2× reaction mixture was composed of 0.4 nM circular DNA template, 0.6 mg mL^{-1} bovine serum albumin, 1 mM dNTPs, 200 nM ROX red dye, 0.01% SYBR Gold, 1 U μL^{-1} murine RNase Inhibitor, 1 U μL^{-1} SUPERase In RNase Inhibitor, 0.05 U μL^{-1} Φ29 DNA Polymerase, and 0.2 U μL^{-1} of Nb.BbvCI nickase in 1× Cutsmart Buffer (50 mM potassium acetate, 20 mM

Tris-acetate, 10 mM magnesium acetate, pH 7.9). The 2× reaction mixture (10 μL) was mixed with samples (10 μL) at 37 °C. Reactions were monitored for 4 hr by fluorescence using a QuantStudio 3 Real-Time PCR System (Applied Biosystems) or Realplex 4S Real-time qPCR Real Time Cycler (Eppendorf). For gel analysis, samples were heat inactivated at 95 °C for 5 min, and stored at –20 °C until use.

IsomiR and Scrambled Sequence Quantification. pg-RCA reactions were performed as described above using miR-375 isomiRs and the scrambled sequence (**Table S1**) diluted to 100 pM in 1× Cutsmart Buffer. A standard curve was generated for fluorescence intensity cutoff time *versus* miR-375.1 concentration from 1 fM to 1 nM in log(10) increments. A logarithmic regression was used to calculate the effective concentration of each isomiR and the scrambled sequence.

Agarose Gel Electrophoresis. Agarose gels were prepared by dissolving 0.5 g of agarose to a final concentration of 0.5% (w/v) in 1× TBE buffer. The mixture was heated to 100 °C, transferred to a horizontal gel electrophoresis apparatus, and solidified for 30 min at room temperature. All samples were prepared with a 6× loading dye, and electrophoresis was performed at 25 V for 1 hr, followed by 50 V for 5 hr. Gels were then incubated for 1 hr at room temperature in a 1:10,000 dilution of SYBR Gold in 1× TBE buffer. Gels were then washed with deionized water and imaged using a Bio-Rad Gel Doc XR+ System with ultraviolet illumination.

Polyacrylamide Gel Electrophoresis. Samples were prepared in 2× TBE-Urea sample buffer and loaded into 10% polyacrylamide TBE-Urea gels in a Mini-PROTEAN Tetra Vertical Electrophoresis Cell with 1× TBE buffer. Electrophoresis was performed at 25 V for 1 hr, followed by 50 V for 2.5 hr. Polyacrylamide gels were stained and imaged as described for agarose gels.

RNA Extraction from Human Plasma. RNA from deidentified and pooled healthy human plasma (Innovative Research, catalog IPLA-N) was extracted using TRIzol LS Reagent according to the manufacturer's protocol. Briefly, 0.75 mL of TRIzol was added to 0.25 mL plasma. Samples were homogenized by pipetting and incubated for 5 min at room temperature. Two-hundred microliters of chloroform was then added to each tube and the biphasic mixtures were allowed to incubate for 3 min before centrifugation for 15 min at 12,000*g*. The aqueous phase was transferred to a new tube and RNA was precipitated with the addition of 0.5 mL isopropanol. After 10 min, samples were centrifuged for 15 min at 12,000*g* at 4 °C. The

supernatant was removed, RNA was resuspended in 75% ethanol, and samples were centrifuged for 5 minutes at 7500*g* at 4 °C. The supernatant was removed and RNA was dried under air for 10 min before resuspension in RNase-free water. Extracted samples were stored at –20 °C until use.

Live Subject Statement. All experiments were performed in accordance with the United States Department of Health and Human Services Policy for Protection of Human Research Subjects. All human subjects work was approved by the Institutional Review Board at the Universityof Illinois Urbana-Champaign and informed consent was obtained for any experimentation with human subjects.

Acknowledgements

This work was supported by the National Institutes of Health (R00CA153914, R01CA227699, and R01CA21209), Department of Defense (W81XWH-15-1-0634), and Mayo-Illinois Alliance.

Supporting Information

The Supporting Information contains: Circular template schematic (Figure S1), gel electrophoresis of circular template (Figure S2), gel electrophoresis of RCA products (Figure S3, S4), RCA fluorescence analysis for reaction parameter optimization (Figure S5, S6), endpoint fluorescence intensity (Figure S7), characterization of sequence specificity (Figure S8), and oligonucleotide sequences (Table S1).

Conflict of Interest Disclosure

The authors declare no competing financial interest.

Author Contributions

L.D.S. contributed to conceptualization, methodology, investigation, data curation, formal analysis, project administration, validation, data visualization, writing the original draft, revision,

and editing. A.M.S contributed to conceptualization, funding, methodology, project administration, resources, supervision, and editing. M.K. contributed to conceptualization, funding, supervision, and editing. S.N. and C.W.K. contributed to investigation, data curation, data visualization, editing, and revisions.

References

1 R. C. Lee, R. L. Feinbaum and V. Ambros, *Cell*, 1993, **75**, 843–54.

2 S. Griffiths-Jones, H. K. Saini, S. van Dongen and A. J. Enright, *Nucleic Acids Res.*, 2008, **36**, D154-8.

3 Y. Wang, R. Lieberman, J. Pan, Q. Zhang, M. Du, P. Zhang, M. Nevalainen, M. Kohli, N. K. Shenoy, H. Meng, M. You and L. Wang, *Mol. Cancer*, 2016, **15**, 70.

4 X. Huang, T. Yuan, M. Liang, M. Du, S. Xia, R. Dittmar, D. Wang, W. See, B. A. Costello, F. Quevedo, W. Tan, D. Nandy, G. H. Bevan, S. Longenbach, Z. Sun, Y. Lu, T. Wang, S. N. Thibodeau, L. Boardman, M. Kohli and L. Wang, *Eur. Urol.*, 2015, **67**, 33–41.

5 P. S. Mitchell, R. K. Parkin, E. M. Kroh, B. R. Fritz, S. K. Wyman, E. L. Pogosova-Agadjanyan, A. Peterson, J. Noteboom, K. C. O'Briant, A. Allen; D. W. Lin, N. Urban, C. W. Drescher, B. S. Knudsen, D. L. Stirewalt, R. Gentleman, R. L. Vessella, P. S. Nelson, D. B. Martin and M. Tewari. *Proc. Natl. Acad. Sci. U. S. A.*, 2008, **105**, 10513–8.

6 H. Wang, R. Peng, J. Wang, Z. Qin and L. Xue, *Clin. Epigenetics*, 2018, **10**, 59.

7 P. Costa-Pinheiro, J. Ramalho-Carvalho, F. Q. Vieira, J. Torres-Ferreira, J. Oliveira, C. S. Gonçalves, B. M. Costa, R. Henrique and C. Jerónimo, *Clin. Epigenetics*, 2015, **7**, 42

8 Z. Wang, M. Gerstein and M. Snyder, *Nat. Rev. Genet.* 2009, **10**, 57–63.

9 E. van Rooij, *Circ. Res.*, 2011, **108**, 219–34.

10 C. C. Pritchard, H. H. Cheng and M. Tewari, *Nat. Rev. Genet.*, 2012, **13**, 358–69.

11 B. W. Buchan and N. A. Ledeboer, *Clin. Microbiol. Rev.*, 2014, **27**, 783–822.

12 L. D. Smith, M. Kohli and A. M. Smith, *J. Am. Chem. Soc.*, 2018, **140**, 13904–12.

13 S. P. Jonstrup, J. Koch and J. Kjems, *RNA*, 2006, **12**, 1747–52.

14 T. Murakami, J. Sumaoka and M. Komiyama, *Nucleic Acids Res.*, **2009**, 37, e19.

15 T. Murakami, J. Sumaoka and M. Komiyama, *Nucleic Acids Res.*, **2012**, 40, e22.

16 H. Liu, L. Li, L. Duan, X. Wang, Y. Xie, L. Tong, Q. Wang and B. Tang, *Anal. Chem.*, 2013, **85**, 7941–7.

17 L. D. Smith, Y. Liu, M. U. Zahid, T. D. Canady, L. Wang, M. Kohli, B. T. Cunningham and A. M. Smith, *ACS Nano*, 2020, **14**, 2324–35.

18 B. Joffroy, Y. O. Uca, D. Prešern, J. P. K. Doye and T. L. Schmidt, *Nucleic Acids Res.*, 2018, **46**, 538–545.

19 Y. Mao, M. Liu, K. Tram, J. Gu, B. J. Salena, Y. Jiang and Y. Li, *Chem. - A Eur. J.*, 2015, **21**, 8069–8074.

20 R. S. Tuma, M. P. Beaudet, X. Jin, L. J. Jones, C.-Y. Cheung, S. Yue and V. L. Singer,

Anal. Biochem., 1999, **268**, 278–288.

21 H. Takahashi, M. Ohkawachi, K. Horio, T. Kobori, T. Aki, Y. Matsumura, Y. Nakashimada and Y. Okamura, *Sci. Rep.*, 2018, **8**, 7770.

22 Z. Williams, I. Z. Ben-Dov, R. Elias, A. Mihailovic, M. Brown, Z. Rosenwaks and T. Tuschl, *Proc. Natl. Acad. Sci. U. S. A.*, 2013, **110**, 4255–60.

23 T. Yuan, X. Huang, M. Woodcock, M. Du, R. Dittmar, Y. Wang, S. Tsai, M. Kohli, L. Boardman, T. Patel and L. Wang, *Sci. Rep.*, 2016, **6**, 19413.

24 J. Duy, J. W. Koehler, A. N. Honko and T. D. Minogue, *BMC Genomics*, 2015, **16**, 95.